A Perceptive Evaluation of Volume Rendering Techniques

Christian Boucheny, Georges-Pierre Bonneau, Jacques Droulez, Guillaume Thibault, Stéphane Ploix

A Perceptive Evaluation of Volume Rendering Techniques

Christian Boucheny Georges-Pierre Bonneau
LJK - Grenoble University - INRIA
and
Jacques Droulez
LPPA - CNRS - Collège de France
and
Guillaume Thibault Stéphane Ploix
EDF

The display of space filling data is still a challenge for the community of visualization. Direct Volume Rendering (DVR) is one of the most important techniques developed to achieve direct perception of such volumetric data. It is based on semi-transparent representations, where the data are accumulated in a depth-dependent order. However, it produces images that may be difficult to understand, and thus several techniques have been proposed so as to improve its effectiveness, using for instance lighting models or simpler representations (e.g. Maximum Intensity Projection). In this paper we present two perceptual studies that question how DVR meets its goals, in either static or dynamic context. We show that a static representation is highly ambiguous, even in simple cases, but this can be counterbalanced by use of dynamic cues, i.e. motion parallax, provided that the rendering parameters are correctly tuned. Besides, perspective projections are demonstrated to provide relevant information to desambiguate depth perception in dynamic displays.

Categories and Subject Descriptors: I.3.3 [**Computer Graphics**]: Picture/Image Generation; I.3.8 [**Computer Graphics**]: Applications; J.2 [**Physical Sciences and Engineering**]:

Additional Key Words and Phrases: Direct Volume Rendering, perception of transparency, static and dynamic cues, Structure from Motion, Perspective projection

1. INTRODUCTION

Dense three-dimensional datasets represent a challenge for the visualization community. Ideally, one would like to see at a glance all the data that fill the space, and have a clear picture in mind of the spatial layout, of the organization within the

Authors' address: [christian.boucheny, georges-pierre.bonneau]@inria.fr, jacques.droulez@college-de-france.fr, [guillaume.thibault, stephane.ploix]@edf.fr

volume of the displayed physical fields. However, such representations are not natural, as the human visual system mainly experiences surfaces that hide one another through occlusion. Thus, early representations of scalar fields were based on the extraction of characteristic surfaces that could be displayed, for instance surfaces of isovalues. But these methods require the viewer to mentally reconstruct a volume from a sequence of pictures, which is a very complex cognitive task.

To overcome this limitation, it has been suggested to consider dense scalar data fields as volumes of particles with emissive and absorptive properties, like drops of water that modify the light rays traversing a cloud. This led to the development of Direct Volume Rendering methods that highly rely on transparencies. These techniques have been throughly developed and improved since their birth in the late 80's. However, it is surprising to notice that they do not seem to be intensively used by final users outside the medical community, as we could observe, despite their implementation in most visualization softwares. As was argued by [Hibbard 2000], "all 3D graphics suffer from ambiguity, with many 3D points projected onto each point of the 2D screen (or of the user's 2D retina). This ambiguity is strongest in volume rendering, where the color of each screen pixel is determined by a (theoretical) continuum of semi-transparent 3D points", which could be one of the main reason why scientists do not find volume rendering to be as accurate as other techniques. Produced images may look nice, but if no recognizable structure is present in the data it can be really hard to extract spatial relationships. Another reason for the lack of interest of scientists in volume rendering consists in the difficulty to tune the Transfer Function (TF), which is the determinant of the final rendering but often proves complex to adjust even for expert users. But strikingly, when [Kaufman and Mueller 2004] give a thorough review of research in volume rendering, none of the near 300 references are devoted to evaluation and validation based on user studies.

In this paper, we address from the human visual system point of view the question of the perceived depth order of semi-transparent objects rendered by means of DVR. The focus is on depth perception, as it is a very important aspect of volume rendering that can be quantified; we do not deal with other perceptive issues such as pattern recognition or matching. To the best of our knowledge, this paper represents the first insight on the perceptive problems of DVR. We do not intend to formulate definitive conclusions, but rather wish to orient future works on volume rendering. Computational costs related to volume rendering of large datasets often lead to quasi-static representations, whereas motion is a strong cue to depth perception. Also, perspective transformations are likely to provide relevant information to remove depth ambiguities. We thus carried out three experiments, in static and dynamic contexts, testing the influence of the projection mode in the latter case. Transparent renderings seem to generate depth order ambiguities, also found in point-based rendering. Our main hypothesis is that if we are able to perceive transparency per se, such as in clouds or water, understanding the spatial layout of data in a translucent material cannot be done in static monocular presentations, but requires dynamic depth cues such as motion parallax. In this paper, monocular will relate to representations without any binocular disparity, like when one looks

at a basic computer screen.

The paper is organized as follows: first, we propose an overall review of Direct Volume Rendering in computer graphics, and present some well-known results about the perception of transparency. Then, in a first experiment, we examine how human subjects are able to discriminate in depth two static objects displayed with DVR technique, when color transparencies and accumulations are the only sources of information. To avoid perspective biases, we use orthographic projections. A second experiment focuses on the perception of depth in rotating semi-transparent volumes, and the effect of perspective projection for such displays is tested in a third study.

2. VOLUME RENDERING IN COMPUTER GRAPHICS

A complete overview of volume rendering is out of scope for this paper. The reader can refer to [Kaufman and Mueller 2004] for a thorough review. In this section we give the main ideas and milestones, and cite the few papers concerned with perception, validation or user studies.

The idea to use transparencies to represent volumetric data has come from initial works on clouds rendering in computer graphics ([Kajiya and Herzen 1984], [Max 1995]). It has been proposed to use the same raytracing techniques to produce images of a volumetric scalar field, considering the field as a density emitter with single level of scattering ([Sabella 1988]). Such representations aim at considering all the data for the display, contrary to what is done in surfacic methods such as isosurface (data thresholding) or cross-section (using cutting planes) renderings that require the viewer to mentally reconstruct the spatial structure of the field seen across a sequence of images.

The basic idea in DVR techniques, whatever their technical implementation might be, consists in an evaluation of the *volume rendering integral*. The luminance corresponding to a ray ω cast from an image pixel and crossing the volume along a segment of length D (with parametrization $x(\lambda)$ along the ray, λ is the distance to the viewpoint and belongs to $[0{:}D]$), is given by:

$$I = \int_0^D C(x(\lambda)).e^{-\int_0^\lambda \tau(x(\lambda')d\lambda')}d\lambda \tag{1}$$

where $C(x)$ represents the voxel color at x, and $\tau(x)$ its extinction coefficient. This equation is often evaluated in back-to-front order based on the following simplification:

$$I \approx \sum_{i=0}^{n} \tilde{C}_i . \prod_{j=0}^{i-1} (1 - \alpha_j) \tag{2}$$

where α_i and $\tilde{C}_i$ stand for the opacity and the color of the i^{th} voxel in the ray. DVR requires the definition of a Transfer Function (TF) ϕ that maps the scalar $s(x)$ associated to voxel x onto luminance l and opacity α values:

$$\phi : s \rightarrow (l, \alpha) \tag{3}$$

The Transfer Function critically determines how the data will be perceived in the final rendering. Its choice may be a very delicate problem, and some efforts have been carried out to automatize this process (for reference, see [Pfister et al. 2000]). Most often, piecewise linear functions are chosen.

Maximum Intensity Projection (MIP) and X-Ray constitute alternatives to optically-based DVR. In the former, only the maximum voxel on each ray is projected on the screen, whereas the later corresponds to an unordered sum of all voxel values along the ray. MIP is very useful for datasets with well-segmented volumes, as is the case with CT or MR medical data (e.g., angiography). MIP and X-Ray tend to generate more contrasted images than DVR, improving the visibility of substructures; but, as they are order-independent, they provide no depth cues to the viewer. Contrary to DVR, images created with X-Ray and MIP have fronto-planar symmetry, which means that volumes viewed from front and back result in the same images.

In computer graphics, a lot of work has been devoted to develop existing techniques, either to reduce the computational costs ([Lacroute and Levoy 1994]) or to better approximate the volume rendering integral and reduce image artifacts ([Engel et al. 2001]). Some works have focused on the improvement of depth perception in volume renderings. [Levoy 1988] implemented a volume rendering pipeline including lighting calculations to strengthen the perception of surfaces within the volume. [Ebert and Rheingans 2000], in their volume illustration framework, introduced NPR techniques such as silhouette enhancement and tone shading in physics-based volume rendering. [Mora and Ebert 2004] suggest to improve MIP and X-Ray using gradient signals inside the volume and stereo-images, whereas [Bruckner and Gröller 2007] introduce halos in the volume rendering pipeline to facilitate depth perception. Generally, improvements are measured on the basis of the quality of produced images, compared with traditional techniques. For instance [Giesen et al. 2007] designed an efficient user study to compare parameters for volume rendering with a metric based on the perceived quality of produced images. Amongst the few user studies led to validate specific volume renderings, we can mention [Kersten et al. 2006], who use atmospheric perspective and stereo to improve X-Ray-like rendering, and [Ropinski et al. 2006] with NPR-enhancement of MIP images in angiography. [Interrante et al. 1997] and more recently [Bair and House 2007] studied how textured-transparent surfaces could convey depth information, but this approach is limited to two wrapped surfaces.

3. THE PERCEPTION OF TRANSPARENCY

Seeing dense and complex transparent media does not correspond to natural situations. We can sometimes look at solid surfaces through translucent media, such as a window or a water surface, or observe complex translucent objects such as clouds or crystals, but in this last case the layout of matter densities inside the volume does not seem obvious.

The perceptual aspects of transparency have been studied for a long time, with particular focus on the required image conditions for producing the illusion of transparent layers. [Metelli 1974] developed a first model postulating that, for a disk

overlapping two vertical strips with different reflectance a and b and producing intersecting areas of reflectance p and q, the level of transparency is given by $\alpha = \frac{p-q}{a-b}$, with values close to 1 leading to full transparency. Interestingly, Metelli's model is firstly experimental and generative, as it corresponds to a disk (the episcotister) with a reflectance t and an open fraction of α that would rotate quickly over the two background strips (leading to $p = \alpha a + (1-\alpha)t$ and $q = \alpha b + (1-\alpha)t$). It can be noted that Metelli's model of perceived transparency corresponds to the widely used alpha-blending equation encountered in computer graphics. Metelli's model was further developed in terms of luminance rather than reflectance by [Gerbino et al. 1990]. More recently, Singh and Anderson [2002; 2004] developed an alternative achromatic model of transparency that relies on Michelson contrasts of adjoining areas. Such variants are required to account for the two aspects of a transparent layer: its luminance and its transmittance, whereas Metelli's model focuses only on the second aspect. As the conditions and ranges of achromatic transparencies have been assessed in many studies (for instance in [Kasrai and Kingdom 2001]), very few works focused on the perceived layout of superimposed transparent media. [Kersten et al. 1992] used two squares separated in depth and rocking back and forth to show that the perceived transparency can bias the depth extracted from motion information, and even alter the impression of a rigid motion.

A fundamental condition for phenomenal transparency - namely the perception of the transparency of a surface - to occur consists in the presence of contour junctions that correspond to luminance steps between adjoining regions. The shape of these junctions (X-, T- or I-junctions) and the layout of luminances around determine if one is likely to perceive transparency, the objects perceived as transparent and thus the spatial layout of the objects ([Anderson 1997]). X-junctions, in which the borders of two objects cross in an 'X' fashion, are considered as the most informative regarding the perception of transparency, as they provide more information about contrast variations between superimposed layers, but T-junctions can also elicit a distinct illusion of transparency ([Masin 2006]). The aforementioned perceptual studies focus on achromatic transparency, i.e. regard objects with a luminance and a transmittance components, but color components can be added in the equations, and conditions for chromatic and achromatic transparencies can be jointly studied, like in [Fulvio et al. 2006].

4. EXPERIMENT 1: STATIC PERCEPTION IN DVR

4.1 Experimental setup

In this first experiment, we question our ability to perceive the spatial layout of volumetric objects rendered through texture-based DVR techniques. We conduct a three-alternative forced-choice experiment in which participants are asked to decide how semi-transparent cylinders are organized in depth. The stimulus we use is intentionally simple, in order to promote transparencies as the unique cue to depth.

4.1.1 *Stimulus description.* The scene stimulus (Figure 1) is composed of two cylinders with different radii and same length, the larger one (LC) being twice

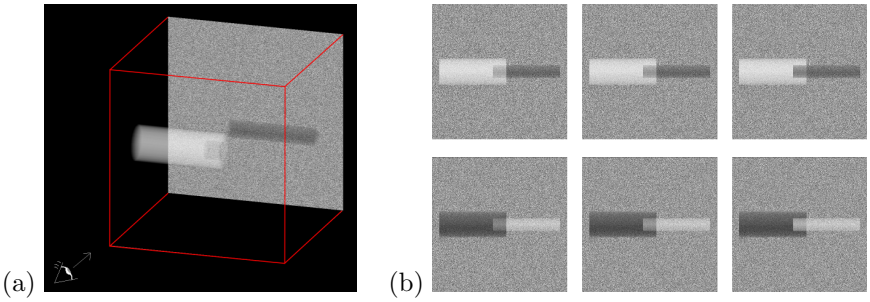

Fig. 1. The two-cylinder stimulus of experiment 1. Figure (a) shows a 3/4 perspective view of the two filled cylinders at different depths, with the large one being empty at its central end. The six main stimuli subjects see during the experiment are illustrated on Figure (b), with the large cylinder being either bright (top) or dark (bottom); for each brightness condition, the large cylinder stands in front (left column) or in the back (right column) of the small one, or the two cylinders are positioned at the same depth (central column).

as thick as the smaller one (SC). In frontal view, the two cylinders lie horizontally, vertically centered; one stands on the left side of the display, the other on the right side. They overlap in image space in a small region that looks like a square-shape intersection area in the middle of the screen. Three dispositions in depth are possible: large cylinder in front of the small cylinder (depth condition $Depth_{large}$), small cylinder in front of the large cylinder ($Depth_{small}$), and the two cylinders at same depth ($Depth_{intersect}$). In this last case, the small cylinder partially extends within the large one.

The two cylinders are filled with a constant scalar value s, making them appear either bright ($s = 1$) or dark ($s = 0.2$). All voxels outside the cylinders are set to $s = 0$, and the part of the LC intersected by SC in frontal view is extruded in all cases, with $s = 0$, so that the intersection image always correspond to the same amount of matter accumulated in depth, whatever the geometric organization of the cylinders might be. Preliminary tests pointed out the need to reinforce the volume appearance of the cylinders when filled with scalar value $s = 0.2$. To achieve this, we simulated pseudo-lighting in the volumes: the scalar value $s(x)$ of a voxel x in a cylinder is given by: $s(x) = s0 + aR(x).L$, where $R(x)$ is the normalized direction of x from cylinder axis and L the direction of a pseudo-light ($s0 = 0.2$ or $s0 = 1$, $a = 0.1$, light coming from above). Values of $s(x)$ are clamped to $[0; 1]$.

There are thus six predefined position conditions for the cylinders: two for laterality (large on the left or on the right) and three for ordering in depth, and two conditions of luminance: LC bright and SC dark, and the converse. Volume data were precomputed on a regular grid, and the required configuration was loaded on a 3D texture before each trial, and displayed in real-time using OpenGL shaders. For rendering, 100 planes regularly spaced out in the scene cube were blended in back to front order. The Transfer Function we use is linear in luminance and constant in alpha: $\phi(s) \rightarrow (s, 0.25)$ (see Section 2).

As mentioned in introduction, we choose to use orthographic projection; this is important, as otherwise the cylinders would vary in apparent size in the different depth configurations, due to linear perspective. Besides, that permits to limit important contour information to a few junctions, which constitute fundamental conditions for phenomenal transparency (see Section 3), and to remove potential 3D mental reconstructions interpolated from apparent sizes and intersections configurations. In our images, only X-junctions and luminance information of the intersection area provide relevant information for decision. Also, in an attempt to limit the influence of the contribution of the background color, we place a white-noise image at the rear; the noise is centered at a value corresponding to the average of screen intensities within dark and bright cylinders (white-noise defined in range $[0.2 : 1]$).

4.1.2 *Experimental procedure.* Subjects are asked for each stimulus to decide how the cylinders are organized in depth. Proposed answers are: "Left cylinder in front", "Two cylinders intersecting", "Right cylinder in front".

During the experiment, subjects' gaze fixations are monitored with an EyeLink®II eyetracking system, that also ensures they are correctly looking at the screen. They sit 0.8 m from a 19-inch LCD screen (resolution 1280x1024), head reposing on a chin-rest. Stimulus image subtends approximately 17° of visual angle, and the intersection of the cylinders 2°. For each participant, a calibration of the eyetracker is performed, then the experiment can start.

An experimental session consists of 5 presentations of each of the 12 possible configurations, the full sequence being randomized. In each of the 60 trials, a red cross first appears in the center of a blank screen, during 1 to 3 seconds (random time). The subject is asked to fixate the cross, then the stimulus is presented for two seconds, followed by the answer screen; gaze positions on the screen are monitored during stimulus display. The subject makes his choice by mouse-clicking on one of the three answers that are displayed on the screen. Then, the next trial starts. At the end of the experiment, subject's reactions and impressions about the task are recorded.

Finally, a small test is carried out, to determine if the difficulty to perform the task can be related to a non-discriminable difference of contrasts between the intersection areas in the different trial configurations. For each of the two luminance conditions (LC dark or LC bright), the three images corresponding to the square intersection area in the separate depth conditions are extracted, and the subject is asked to order these images from brighter- to darker-looking. As these images correspond only to the cylinders intersection area, and thus do not contain any transparency cues, subjects are not disturbed by the depth judgments they have made previously. All subjects answered immediately and correctly.

Stimulus presentations last 2 seconds each. A pilot study showed that longer times (we tested 5 seconds duration) bias answers. From our observations, subjects elaborate more complex per- and between-image cognitive strategies. We thus reduced presentation times to 2 seconds, in an attempt to reinforce the part of perception against conceptual reasoning in subjects' decisions, as we focus on the ability of the

human visual system to perceive depth-organization of semi-transparent objects.

4.1.3 *Participants.* Ten subjects, ranging in age from 22 to 39, participated in the experiment. They were all naive as to the goals of the study, and only two of them had experience with volume rendering. All had normal or corrected-to-normal vision. Before they went through the true trial sequence, they read the experimental protocol, practiced on a few trials without head-tracking (trials order differed from the real experience) and then were shown again top-front three-quarter views of some of the stimuli (Figure 1, (a)). This ensured they correctly understood the task, and would keep in mind all the geometric and volumetric properties of the stimuli.

4.2 Results

Overall and per-condition mean performances are computed for each participant. Four of the 10 subjects passed a second experimental session with a different trials order after a few minutes break. In this case, we compute the average scores for the two sessions considered as one; we thus end with 10 result sheets.

Averages are illustrated in Figure 2(a). In this depth-ordering task, subject performances are low, with only 48,1% average correct answers, but clearly above chance level (Student's t-test, $p < 0.01$). If we analyze the results with respect to depth configuration, we notice levels of 71% for case $Depth_{large}$, 29.3% for $Depth_{small}$ and 44% for $Depth_{intersect}$. These results are above chance-level when the large cylinder is presented in front of the small ($p < 0.01$) or when the two intersect, but not when the small lies in front of the scene.

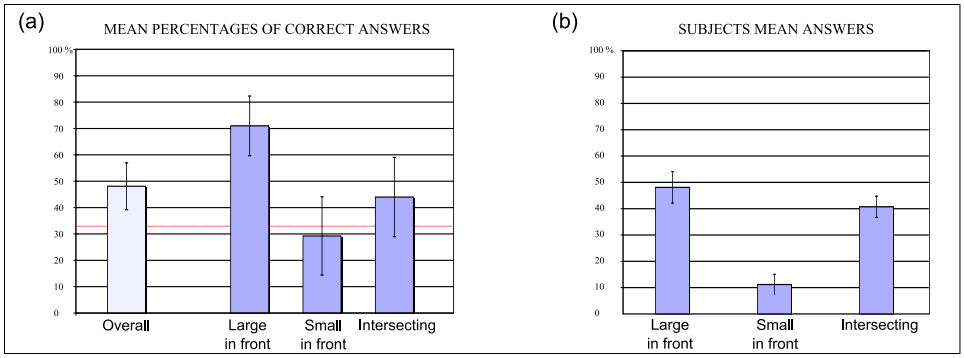

Fig. 2. (a) Mean correct answers averaged over all participants and detailed for the three depth configuration in experiment 1. Error bars represent 95% confidence intervals. Participants overall performances were low, only slightly above chance level. More correct answers are recorded when the large cylinder lies in front, whereas guesses for the small cylinder in front do not differentiate from chance. Intersecting cylinders were detected with little more than chance level. (b) Participants mean answers for the three depth configurations in experiment 1. Error bars represent 95% confidence interval. An important bias towards seeing the large cylinder in front can be noticed, whereas subjects are less keen on placing the small cylinder closer to the eye.

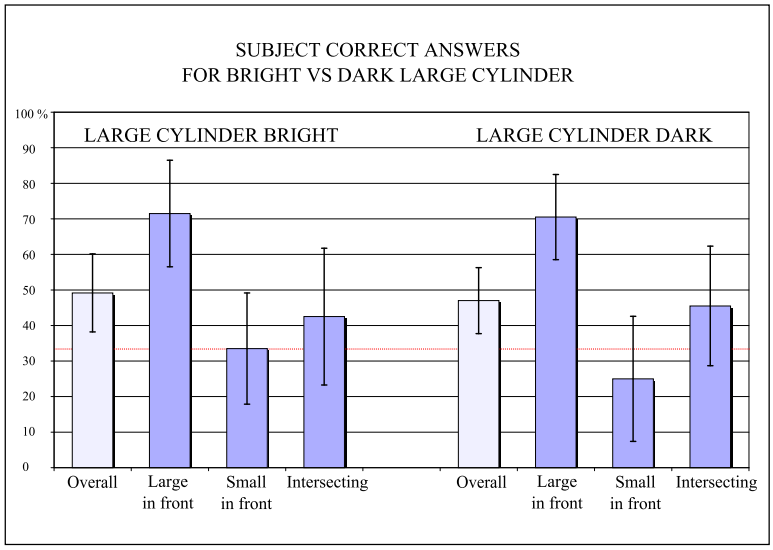

Fig. 3. In experiment 1, mean correct answers are coherent across the two brightness conditions (large cylinder bright or dark).

A first explanation of these global results can be found in the mean reported answers (Figure 2(b)). In the experiment, participants are biased toward seeing the large cylinder in front of the display (48.4% of all answers) or the two cylinders intersecting (40.4%), and reluctant to imagine the small cylinder lying closer to the eye (only 11.2% of answers). We also investigated if the respective luminosity of the two cylinders have any influence on subjects' choices, but performances when the large cylinder appears dark or bright look very similar (Figure 3).

It could be argued at first sight that the globally low level of answers giving the small cylinder closer to the eye can be explained by the fact that the large cylinder, occupying more screen space (twice as much as the small does), is likelier to attract viewer's attention, which could force "large in front" answers. However, a visual analysis of participants' gaze trajectories during the trials reveals that in average more saccades fall into the small cylinder than into the large. Four types of ocular trajectories are mainly observed: fixations limited to the intersection area (EM_{in}), center-to-small cylinder exploration (EM_{small}), center-to-large cylinder exploration (EM_{large}) and between-cylinders exploration (EM_{both}). Examples of each category are illustrated on Figure 4. For all subjects but one, EM_{small} dominate over EM_{large}, with an approximate 3:1 average ratio ($\overline{EM}_{small} = 15.1$ and $\overline{EM}_{large} = 5.2$, with 60 trials per experiment). EM_{large} and EM_{both} are globally equal in size, but with noticeable between-subjects disparities. Gaze fixations limited to the central intersection area represent approximately half of the trials; they generally correspond to a fixation of either the lateral borders of the cylinder, either one of the two X-junctions present in the stimulus.

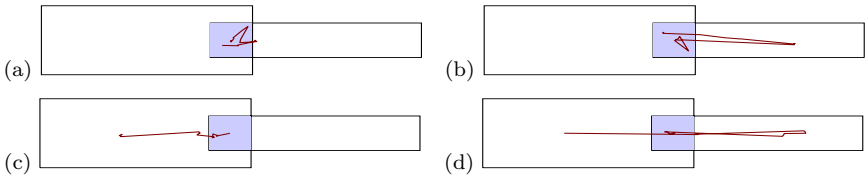

Fig. 4. Examples of the main gaze profiles recorded across trials in experiment 1. Subjects would focus on the intersection area (a), or visit the small (b) or the large (c) cylinder exclusively, or jump from one to another (d).

4.3 Discussion

In this experiment, we try to evaluate our visual ability to perceive the correct organization in depth of semi-transparent objects presented statically and rendered through DVR. Such static presentations are likely to occur for large datasets in scientific visualization, due to the computational costs associated with DVR. The stimulus we use is very simple and results in images that clearly differentiate in regard to contrast, but overall performances prove to be relatively poor, although above chance-level. Results collected in this experiment show that our perception of the organization in depth of overlapping semi-transparent objects is weak, and influenced by factors other than the sole combination of luminances.

Useful visual information is limited to contrast levels at objects borders and intersections, mainly at the central ends of both cylinders. Orthographic projection eliminates all potential geometric cues. The stimulus was chosen as simple as possible to reduce the influence of complex cognitive strategies on the results. Scenes built from more complex objects may reveal more borders, but the relative spatial continuity of the data often leads to a blurring of these information that weakens even more depth perception.

Thus, traditional static transparent renderings may not appear as effective candidates to provide a clear understanding of the spatial structure of a volumetric dataset, even if the rendering equation takes into account the depth ordering of the data, as DVR does.

Some factors might explain at least part of our results. Firstly, the stimulus we use is highly asymmetric, due to the difference in size of the two cylinders. We tried to compensate for this point by alternatively presenting the large cylinder on the left and on the right of the display. On the other hand, this asymmetry is a desired artifact, as it provides viewers with two X-junctions, a very important cue to transparency (see Section 3). These X-junctions correspond in our case to the intersections between the vertical end of the large cylinder and the horizontal limit of the small cylinder. Subjects may be biased toward seeing the X-junctions as the unique transparency border, whereas the central end of the small cylinder is also a transparency border itself. An overview of gaze trajectories limited to the intersection area make us think this is not the case, but we cannot be totally confident on this point. If subjects find it easier – consciously or not – to interpret the image as containing only one transparent cylinder, the fact that at the X-

junction the horizontal border of the small cylinder is larger than the vertical border of the large cylinder might facilitate the perception of LC as more transparent than SC. Also, the large cylinder offers a wider surface through which more background details can be seen, which might strengthen this effect. And if only one cylinder is perceived as transparent, then it will definitely appear in front of the other.

By reducing stimulus presentation time to only two seconds, we wished to limit as much as possible the influence of more cognitive approaches in the decision process. However, these cannot be totally rejected, as post-experiment introspective questions showed. For instance, many participants reported that one stimulus often influenced the decision they made for the following, which was possible when consecutive stimuli were close enough (only depth condition modified). On the other hand, all but two participants also stated that they were highly uncertain about the answers they gave, and that consecutive stimuli could as well disturb them about previous answers they gave. The limited presentation time also restricts the possibility to build firmly anchored strategy based on progressive classification of the luminance configurations. We cannot reject the assumption that short-term memory plays a role in the present experiment, but its effect is not expected to modify consistently the recorded performances.

Answer times were monitored during the experiment, but not taken into account for the analysis. Subjects were however instructed to answer as fast as possible, which was generally the case (average answer time: 1.9 seconds), but no mechanism was introduced to force quick answers. However, mean reaction times show no linear correlation with overall performances ($R^2 = 10^{-4}$). We observed a limited bias during experimental sessions, with participants sometimes positioning the mouse on the answer corresponding to "small in front", and then switching to another choice.

5. EXPERIMENT 2: IMPORTANCE OF DYNAMIC INFORMATION IN DIFFERENT DVR TECHNIQUES

Experiment 1 focuses on the perception of depth order of semi-transparent objects displayed statically. However, it has been known for a long time now that we can recover the three-dimensional structure of an object projected on a 2D screen when a perspective motion is applied to it. This ability to perceive 3D structures from 2D velocity fields has been labeled the Kinetic Depth Effect (KDE, [Wallach and O'Connell 1953]) or recovery of Structure from Motion (SfM, [Ullman 1979]). Stimuli based on a weak perspective or parallel projection are likely to induce a bistable perception, as in the Necker cube : the object is either seen in its correct configuration and rotating direction or inverted in depth with and opposite motion. An observer viewing the stimulus continuously rotating will often experience randomly occuring reversals of the rotation direction and object configuration. Extraction of structure from motion can be influenced by other visual cues, such as stereopsis (e.g. [Nawrot and Blake 1989]), but the interplay between transparency and motion information has not been thoroughly studied, as most of the works related to KDE implement point clouds or wire objects. [Kersten et al. 1992] studied how phenom-

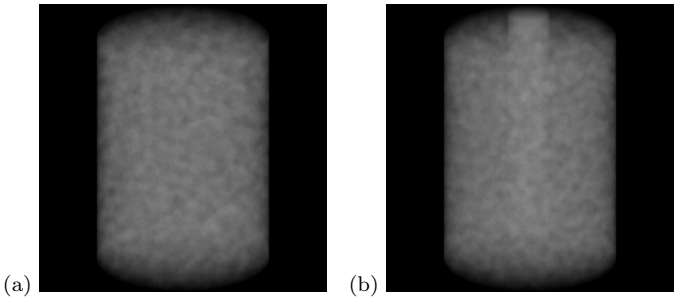

Fig. 5. The rotating cylinder filled with Perlin noise used in experiment 2, seen from top, with DVR rendering (a). To choose acceptable rendering parameters, we required that a sub-cylinder filled with maximal value be always visible (b).

enal transparency can alter the perception in depth of two overlapping squares, and [Kersten et al. 2006] analyzed the influence of stereo and atmospheric perspective to improve the perception of depth in the X-RAY rendering of a rotating cylinder.

In this second experiment, we look at how volume rendering techniques can convey information about the spatial layout of the supported data in a dynamic context. More precisely, we test the influence of the Transfer Function that associates an opacity and a luminance to every voxel scalar value in order-dependent DVR (see Section 2), and compare performances to order-independent methods, namely X-Ray and MIP. We try to measure the conditions for volume rendering techniques to provide non-ambiguous depth cues in a dynamic display. MIP and X-Ray can be faster techniques, as they don't require any ordering of data in depth, but as such they don't provide any depth cues, which produces strong ambiguities in the display.

5.1 Experimental setup

5.1.1 *Stimulus description.* For all rendering conditions, the same stimulus is used, based on [Kersten et al. 2006] previous work: a vertical cylinder, orthographically projected on the screen, rotates either to the left or to the right in frontal view (rotation speed: $34°/s$). The cylinder is filled with volume data generated from Perlin noise functions [Perlin 1985], while exterior is set to 0. The advantage of this function is to provide non-homogeneous data that vary continuously, without any identifiable structures in the volume that could cognitively bias subject's decisions. The Perlin noise value $P(x)$ in a voxel x is defined by:

$$P(x) = \sum_{i=0}^{n-1} \frac{N(b^i x)}{a^i} \tag{4}$$

where $N(x)$ is the basic Perlin noise function, and b and $1/a$ define the relative frequency and persistence of the summed harmonics, respectively. We chose $a = b = 2$ and $n = 4$. Volume data are stored in a 3D texture, and rendering is performed through 100 planes accumulated back to front. Animation images of the rotating cylinders are precomputed, to guarantee that the stimuli will effectively

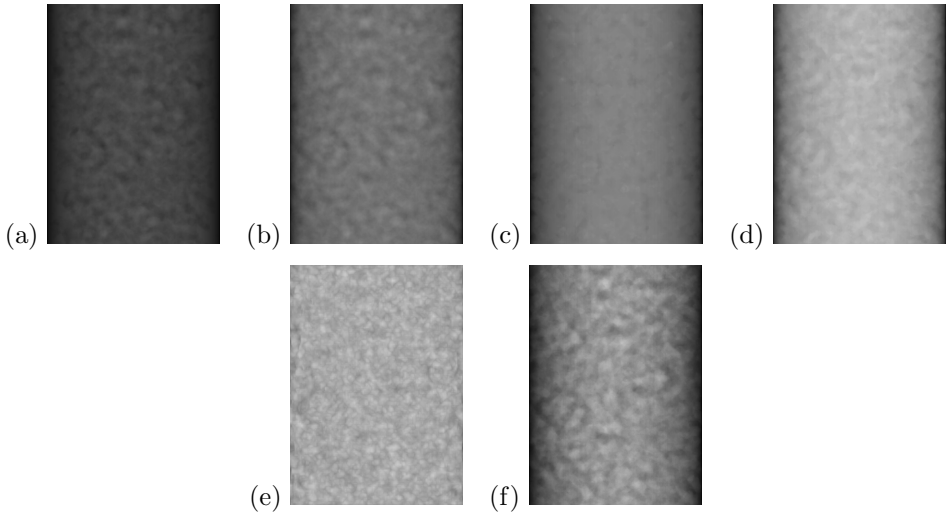

Fig. 6. The 6 cylinder renderings implemented in experiment 2, in frontal view. (a) and (b) correspond to DVR with TF linear in luminance (conditions $DVR1$ and $DVR2$), (c) and (d) to DVR with TF linear in opacity (conditions $DVR3$ and $DVR4$), (e) is MIP rendering and (f) X-Ray.

be presented with a constant refresh rate of 60 images/s. The display appears as a flat rectangle in a static presentation, but motion generates the impression of a rotating cylinder through KDE. The experienced motion direction (clockwise or counter-clockwise) straightly correlates with perception of depth within the volume.

Six rendering conditions are defined: X-Ray, MIP and four DVR with different parameters for the Transfer Function. TF tuning remains a very delicate problem in volume rendering, due to the huge number of candidates. In this experiment, we decided to test two particular cases, one Transfer Function linear in luminance (which we will refer to as DVR_l), the other linear in opacity (DVR_α):

$$(DVR_l)\ \ l(s) = s\ \ ,\ \ \alpha(s) = \alpha_l \tag{5}$$

$$(DVR_\alpha)\ \ l(s) = 1\ \ ,\ \ \alpha(s) = \alpha_a s \tag{6}$$

Two values are chosen for α in each condition, based on a simple transparency test: we placed inside our main cylinder, tangent to its border, a small cylinder of same height but four times less thick. Scalars inside this test cylinder were given a value of 1, and values of α were chosen such that this cylinder could be seen when located in front and at the rear of the main cylinder. This approximately corresponds to situations where maximal values can always be perceived, no matter where they stand. We ended with $\alpha_l = 0.01$ and $\alpha_l = 0.025$ in DVR_l condition, and $\alpha_a = 0.015$ and $\alpha_a = 0.025$ in DVR_α condition. We will further refer to these conditions as $DVR1$ and $DVR2$ (DVR_l equations), and $DVR3$ and $DVR4$ ((DVR_α equations)), respectively.

Each of the six rendering conditions is implemented for a cylinder rotating to the

left and to the right of the display, which results in 12 conditions.

5.1.2 *Experimental procedure.* Subjects are asked to determine the perceived direction of rotation of the cylinder, by clicking with the mouse on the icon corresponding to their choice (either "to the left" or "to the right", as they could perceive it for the 'front surface' of the volume).

Experimental setup is the same as in experiment 1 (Section 4.1.2), with subject's gaze position tracked during stimulus presentation. The rotating cylinder occupies 14° fov vertically, 10° fov horizontally, resulting in a maximum speed of $3°/s$ in visual field.

An experimental session consists of 5 presentations of each of the 12 possible configurations, the sequence of trials being randomized. Each of the 60 trials starts with the red cross fixation, followed by a presentation of the rotating stimulus in one of the defined conditions. After 0.5 second, the answer screen is displayed and the subject decides the rotation direction. Then the following trial immediately starts. At the end of the experiment, subject's reactions and impressions about the task are recorded.

The short presentation time – half a second – prevents the occurence of reversals.This eliminates the influence of perception bias in case of ambiguities; for instance, if two directions were successively experienced for the same stimulus, then one might tend to answer more frequently "to the right" than the converse. Such a preference has been noticed in the experiment, with 65% answers corresponding to "to the right".

5.2 Results

Ten subjects participated in this experiment, the same who volunteered for experiment 1.

Performances for MIP and X-Ray conditions are very close to chance-level (48% and 54% correct answers, respectively), which is not a surprise as they don't provide viewers with any depth cues, being order-independent techniques. This validates that our stimulus does not include any cue that can be used to solve the task.

DVR leads to very different performance levels, depending on the nature of the implemented TF. Condition DVR_l (α constant) presents no ambiguity, with 99.5% correct answers. On the contrary, performances for an alpha linear with respect to the scalar value are much more contrasted, with 11% and 79% correct answers for conditions $DVR3$ ($\alpha(s) = 0.015$) and $DVR4$ ($\alpha(s) = 0.025$), respectively. The value 0.015 shows a strong ambiguity in the visual display, as performances lie far below chance level, which can be interpreted as: "data at the rear of the volume are perceived closer to the eye as those in front". A value of 0.025 reveals more correct depth perception within the volume, but this rendering is still prone to ambiguities, as performances clearly differentiate from perfection (Student's t-test, $p < 0.01$).

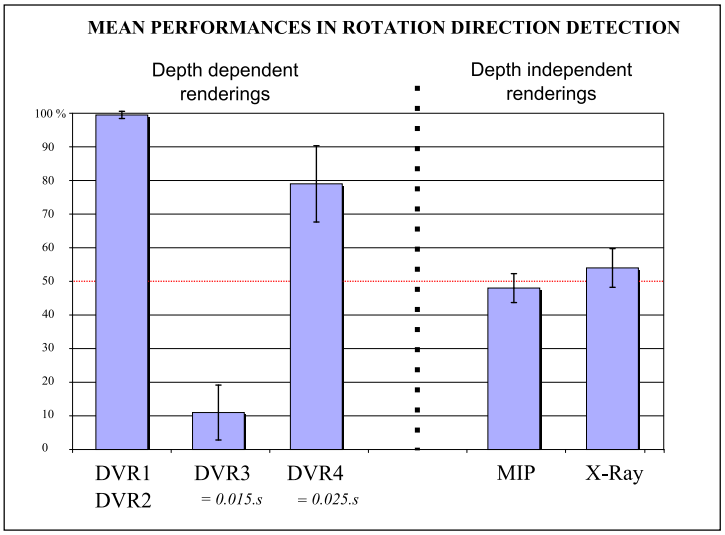

Fig. 7. Correct answers in experiment 2 for the different rendering conditions, with pooling over both levels for DVR_l. Only DVR with luminance-based Transfer Function provide non-ambiguous depth perception within the cylinder, whereas linear-alpha TF can be highly unreliable.

5.3 Discussion

Results obtained in this experiment prove that in a dynamic context DVR can lead to a strong perception of the organization in depth of volumetric data, but that this can be achieved only through a careful tuning of the Transfer Function (TF). Given the size of potential TF space (for integer scalar values in range [0:255] mapped to 1-byte luminance and 1-byte alpha, there are already $(256 * 256)^{256}$ possibilities !), we restricted our analysis to as few as two TF sub-classes, those linear in luminance and constant in opacity, and the converse. We have shown that the former produce reliable renderings, whereas the latter are more prone to elicit ambiguous perception of the spatial layout of the data. In general cases, the tuning of the TF is a very complex problem that is solved empirically, even if some attempts to propose automatic methods have been proposed (for reference, see [Pfister et al. 2000]). Today TF are getting more and more complex; non-linearities are often introduced, as well as multiple dimensions. Our results, obtained on the very simple case of linear unidimensional functions, cannot be easily generalized to all potential TF. However, we explicitly show that, even for order-dependent volume rendering, a Transfer Function resulting in a correct discrimination of objects within a volume can disturb our perception of the spatial layout of these objects.

The different techniques and sets of parameters produce renderings with different contrast ratios, that were not equalized over the conditions (see Table I). This could be a factor modifying the perception of the cylinder motion. For instance, a moving target with very low contrast is likely to embed areas seen as flat in luminance, and fixations to such patterns would lead to a percept close to immobility. In the present experiment, however, participants reported that they always perceived

Rendering	MIP	X-Ray	DVR_1	DVR_2	DVR_3	DVR_4
Mean pixel intensity (in [0:255])	170	145	73	114	128	176
Michelson contrast	0.174	0.235	0.219	0.155	0.1245	0.113

Table I. Michelson contrasts for the different renderings implemented in experiment 2.

motion, and only few of them felt that speed might have varied across trials, with slower rotations in condition $DVR3$, which of course was not the case.

6. EXPERIMENT 3: THE INFLUENCE OF PROJECTION FOR DEPTH PERCEPTION IN A DYNAMIC CONTEXT

In experiment 2, we voluntary restricted our study to parallel projection, in order to limit available depth information to the accumumation of transparencies. Indeed, most studies about the kinetic depth effect make use of parallel projections, with the observation that linear pespective constitutes a reasonable approximation of parallel projection for small visual angles. However, if this condition is suitable to elicit a three-dimensional percept, the perceived depth in the display often appears ambiguous. A bistable state exists, and subjects are likely to perceive reversals of the rotation direction and depth order while continuously observing the motion.

Replacing parallel by perspective projection is likely to positively impact one's ability to make correct depth judgments, due to the modification of projected velocities in the display induced by perspective foreshortening. Indeed, [Rogers and Rogers 1992] observed a clear disambiguation by perspective in a task of depth judgment on translating bands of dots. [Eagle and Hogervorst 1999] pointed out that subjects better discriminate dihedral angles between two sheets in rotation for large displays with perspective projection. More recently, [Petersik and Dannemiller 2004] presented to naive observers a rotating sphere filled with dots and sometimes reversed its rotation direction during the motion; using different levels of perspective, they demonstrated that the average number of correctly perceived switch of rotation direction was clearly influenced by the selected projection.

In the present experiment, we thus test how the use of a natural or exaggerated perspective projection can facilitate the correct perception of depth in ambiguous transparent renderings. We also implement renderings based on dots to bridge the gap with stimuli traditionnally found in KDE-SfM litterature.

6.1 Experimental setup

6.1.1 *Stimulus description.* The stimulus is basically the same as in experiment 2, consisting of a cylinder filled with Perlin noise, with the six volume renderings illustrated in Figure 6. Two rendering conditions are added to the previously described ones, based on classical stimuli used in KDE experiments (e.g. [Green 1961]). They consist of 2000 white solid dots (one-pixel size) randomly positioned either on the surface of the cylinder (condition CLOUD-SURF) or inside the volume (condition

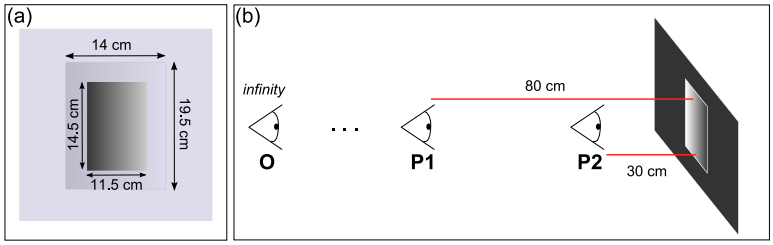

Fig. 8. (a) To limit information extracted from borders in non-orthographic viewing, only the central part of the cylinder is visible, whereas the rest of the display is masked by a black window (displayed in transparent-blue in the picture). (b) Three projections conditions are used, corresponding to a virtual viewer placed at infinity (O), 0.8 m (P1) and 0.3 m (P2) from the cylinder.

CLOUD-VOL). In addition to the orthographic projection (O) implemented in experiment 2, we also built two perspective views of the cylinder, corresponding in subject's space to a viewing distance of approximately 80 cm (condition P1, approximation of a natural perspective for the viewer) and 30 cm (condition P2, amplified perspective). Perspective projection generates a noticeable difference of speeds between voxels lying at the rear and at the front of the object, which provides subjects with an additional kinetic depth cue. The ratio of maximal rear and front speeds at screen were computed to be 0.86 and 0.62 in condition P1 and P2, respectively. The virtual positions of the viewer are explicited in Figure 8(b).

The new perspective conditions imply that top and bottom surfaces of the cylinder are visible on screen for transparent renderings. This new information would probably provide subjects with artifactual cues for detecting the rotation direction, as well as perturbate them when jumping from one trial to the following. To limit such object-structure biases, the extremities of the volume are masked, as illustrated in Figure 8(a), so that only the same on-screen center part of the cylinder remains visible in each display. As a consequence, it must be noted that some of the relevant information for perceptual decision might be removed, which importance cannot be assessed in advance.

6.1.2 *Testing for artifactual 2D cues.* In conditions P1 and P2, due to the perspective projection, elements of the volume placed closer to the viewer will move faster on screen than those located at the rear. This is the key information that one can use to remove any ambiguity in depth perception, like those arising in experiment 2 for MIP and XRAY renderings. However, due to the structure of our stimulus, this also results in an average horizontal screen-speed of the volume biased towards the direction of rotation of the front surface. As stated by [Sperling and Landy 1989], we cannot exclude that subjects would answer, consciously or not, on the basis of this 2D artifactual pattern, thus ignoring or not perceiving the 3D structure of the displayed stimulus.

To assess this, we add to the main experimental session test trials in which a horizontal translation of the cylinder opposes the rotation bias. These tests are implemented in the amplified perspective display (P2), for the volumetric cloud

(CLOUD-VOL). Three translation conditions are defined: no translation at all (T0), a translation that nulls the mean velocity of the cloud on screen (T1) and a translation that equalizes the absolute values of maximal rear and front projected speeds (T2). As the cylinder in perspective is clipped by the rectangular mask, more points can be seen at the rear of the volume than in front, so that condition T2 leads to an inverted mean speed on screen (if subjects are guided by the average screen-speed of points, they are likely to give false answers). Details of the computations of the translation are given in Appendix A.

These test conditions are presented to the subjects in two equivalent blocks, before and after the main session. Each block contains 5 trials per condition and per rotation direction, which results in 30 randomized trials. Among the potential reasons for errors in these sessions, errors at the beginning will probably reveal a global difficulty with the task while errors at the end might stem from visual tiredness.

6.1.3 *Experimental procedure.* As in experiment 2, subjects are asked to determine the perceived direction of rotation of the cylinder, by clicking with the mouse on the icon corresponding to their choice. They sit 0.8 m from a 19-inch LCD screen (resolution 1280x1024), but contrary to previous experiments their gaze was not tracked in the present study. No feedback about performances is provided during the experiment. Before the experiment starts, subjects are explained the task through the presentation of a solid rotating cylinder, and they are told that the number of trials with 'to the right' and 'to the left' rotations are not necessarily equalized, in an attempt to limit hysteresis biases. Also, subjects are explicitly asked to answer as quickly as possible, on the basis of their first visual impression. These two points are made clear so as to limit as much as possible the influence of perceptual reasoning in the construction of the answers.

The visible part of the cylinder through the mask, not depending on the projection, occupies 10.4° fov vertically and 8.4° fov horizontally.

An experimental session consists of 3 blocks of trials: beginning test session, main session and end test session. Breaks are programmed between sessions, and in the middle of the main session to impede the occurrence of visual fatigue. The main session gathers 240 randomized trials, each configuration (rotation direction x rendering x perspective) being presented 5 times. Each trial consists of a red fixation cross followed by a 0.5 s presention of the stimulus followed by the answer screen. When the subject makes his decision, the following trial starts.

At the end of the experiment, subject's reactions and impressions about the task are recorded. In particular, the subject is asked if he perceived more rotations in a specific direction, if the rotation speed appeared constant between trials and if a special motion was detected during the test trials.

6.1.4 *Participants.* Twenty four new subjects, ranging in age from 22 to 58, participated in this experiment. They were all naive as to the goals of the study, and presented a great variability of expertise regarding general 3D graphics, from totally

naive to daily users. All had normal or corrected-to-normal vision.

6.2 Results

Overall, increasing perspective distortions clearly leads to a facilitation of the perception of the correct depth ordering within the volume, as illustrated by Figure 9. To assess this, we perform a series of Wilcoxon oriented tests to compare for each rendering paired conditions P1 vs O and P2 vs P1, with the respective alternative hypotheses: $P1 > O$ and $P2 > P1$. Except for DVR1 and DVR2 conditions, for which orthographic projection already stands as unambiguous, all tests are significative at 5% level. For renderings that do not provide any depth cue in orthographic projection, namely MIP, X-RAY, CLOUD-SURF and CLOUD-VOL, baseline performances consistently lie around the 50% chance level. Regarding DVR3 and DVR4, mean results in O-projection clearly differ from those obtained earlier (see Section 5.2 and Figure 7), with 38.7% and 53.3% correct answers this time against 11% and 79% in experiment 2, respectively. This discrepancy might reveal an increased diffilculty to perform the task due to the mask hiding important information at the lateral sides of the cylinder in these renderings.

The importance of the perspective factor highly depends on the rendering condition, as shown in Figure 10. For instance, performances for the volumetric cloud rendering increase almost linearly up to 94.6% correctness in P2 condition where the surfacic stimulus exhibits only 73.5% mean correct answers. Performances for DVR4 highly resemble those of CLOUD-SURF, while those for DVR3 always lie under the others. MIP and X-RAY exhibit more complex bahaviours. The former clearly benefits from a light perspective (P1), following CLOUD-VOL with performances significantly above DVR4, CLOUD-SURF and X-RAY (Wilcoxon paired test, p=0.037), but increasing the perspective produces only little improvement (P2). On the contrary, X-RAY rendering is significantly affected by an exaggerated perspective (P2) where it significantly outperforms MIP (p=0.036).

The tests explicited in Section 6.1.2 show high performances: in average 95.2%, 93.8% and 93.3% before the experiment for T0, T1 and T2 translation conditions, respectively, and 97.1%, 95.7% and 94.3% at the end. These data remain close to the 94.6% average observed for CLOUD-VOL in P2 projection during the central experiment. This demonstrates that subjects clearly understood the task, and at least for this rendering condition answered on the basis of a three-dimensional perception, which reveals a true KDE effect. None of the participants but one noticed the additional translation in some of the trials.

6.3 Discussion

Perspective foreshortening induces a difference in projected velocities, and the present experiment shows that subjects are able to use this cue to disambiguate the volume they see rotating, independently of the rendering. For X-RAY, this result complements the work by [Kersten et al. 2006] who tested the influence of stereo and atmospheric perspective on kinetic depth perception. It must be noted that perspective plays a role even when the rendering does not provide substructures

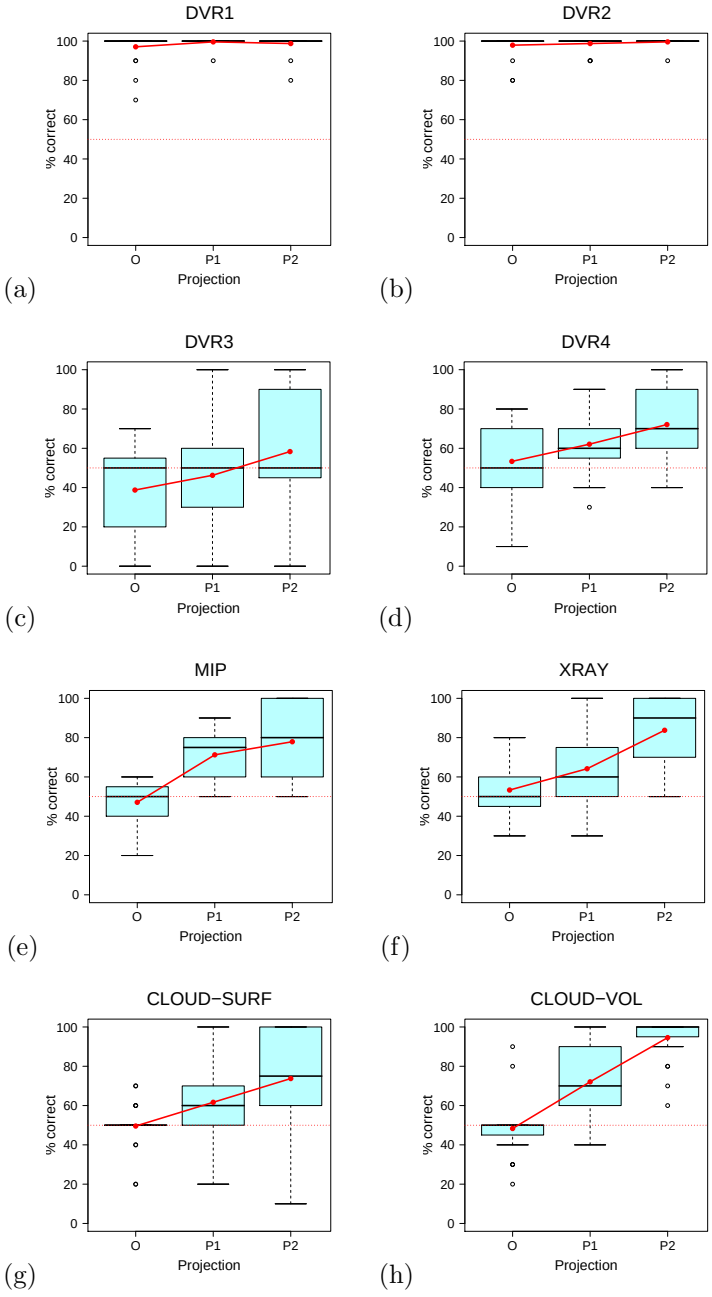

Fig. 9. Subjects performances for each rendering. Box-and-whisker diagrams emphasize the variability of the results through the population (median, lower and upper quartiles and outliers), whereas the red lines describe the evolution of mean performances in the three projection conditions. The projection mode reveals a clear influence whose strength greatly varies across renderings.

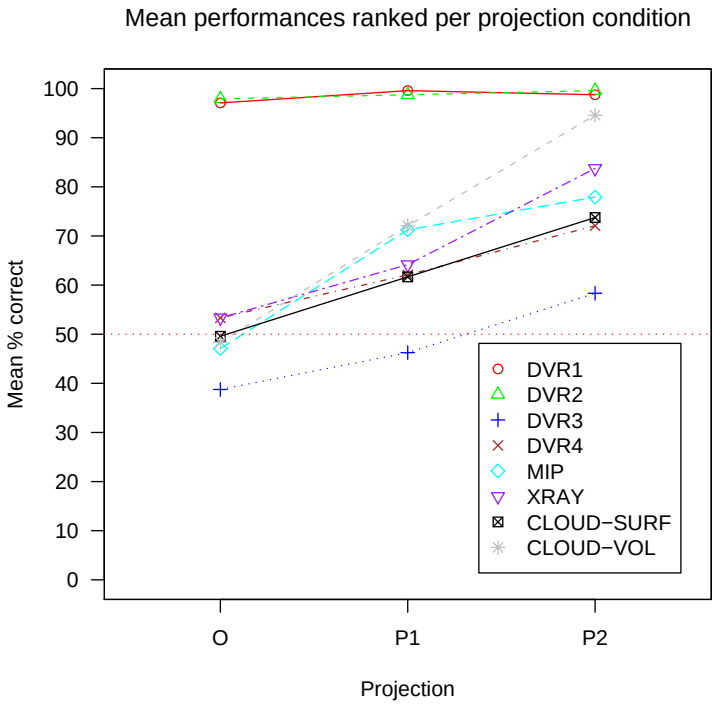

Fig. 10. Mean performances for each rendering plotted against projection condition.

within the domain looking solid and stable in time, as is the case for all volume rendering techniques, and especially MIP and X-RAY. This is coherent with the work by [Todd 1985] who reported that KDE does not require projective correspondance in the display along the motion, and is quite robust to noise.

However, the effect of perspective greatly varies across rendering conditions and subjects. Of particular interest, surfacic and volumetric point clouds are perceived very differently, the later presenting better depth discrimination than the former, and appear to enclose average results for MIP and X-RAY. With the Perlin noise implemented in the experiment, MIP rendering appears as sensitive as a volumetric cloud of points to a light perspective (P1), but then exaggerating the projection deformation has less impact than for points in the volume; this might be due to the very noisy appearance of this rendering, sometimes described as a "'bunch of evanescent snowballs"'. The impact of exaggerated perspective on XRAY may sound quite surprising, as this rendering presents a very blurry, confusing image; it may reveals subjects' ability to rely also on second-order motion to compute depth information.

The variability in the results of this experiment can be partially explained by the fact that subject are very often biased toward seeing a specific rotation direction in

case of relative ambiguity. For instance, the cylinder in O or P1 projections will be more often perceived as rotating couterclockwise by some subjects, and clockwise by others, independently of the actual motion. We measured for cloud renderings the correlation between the strength of this bias (measured for a subject and rendering condition as the maximal number of answers in a particular direction, either righ or left) and the overall number of correct answers, and found non-neglictible links for CLOUD-SURF and CLOUD-VOL in P1 projection with $R = -0.65$ and $R = -0.67$ (Spearman's rank correlation coefficient). This means that a subject's natural preference for a specific rotation direction is sometimes a strong effect that limits the impact of perspective cues for correct depth judgments. Though this effect has been reported earlier (e.g. in [Sereno and Sereno 1999]), we are not aware of any explanations about it.

To disrupt shape information present in the top and bottom borders of the cylinder in non-orthographic projections, we implemented a mask revealing only the central part of the cylinder. However, this mask also increased the complexity of the task, as can be seen from the difference in orthograhic projection performances for DVR3 and DVR4 compared to results in experiment 2. Also, subjects reported that they sometimes perceived more a blurry 2D stimulus composed of floating surfaces than a real 3D cylinder. Tests performed before and after the main experiment demonstrated that sujects performed the task on the basis of a 3D perception for the volumetric cloud in exaggerated perspective, but we cannot assert this is always the case for other conditions.

7. GENERAL DISCUSSION AND CONCLUSION

The display of space filling data remains a challenge, as it requires on the one hand to find renderings that does not hide much of the data to the viewer, which is the main drawback of surfacic techniques, while unambiguously unveiling the organization in depth of these data. Various methods have been proposed, the major class being based on physical (optical) models. However complex and informative they might appear, these renderings implicitly assume that the human visual system produces accurate perceptions of transparent volumes, whereas we seldom face such visual images in our daily life. Interestingly, we find the same physical roots in early psychological works on the perception of transparency, that were based on the experimental framework of the episcotister. But, as mentioned by [Singh and Anderson 2002], the relationship between perceptual theory and generative models is often left rather vague, and their experimental work emphasizes the deviation between perceptual transparency and Metelli's episcotister model. In a similar way, we showed that using models of light propagation in dense matter does not necessarily elicit a correct perception of the spatial layout of even simple structures through static presentations. Indeed, it appeared that the human visual system is not tuned to interpret correctly such representations, and may be strongly biased.

Nevertheless, these order-dependent methods operate reasonably well in a dynamic context, provided that Transfer Functions are carefully chosen. Exaggerating the perspective proved to be quite efficient in disambiguating depth perception, even

for order-independent methods. These results underly the need to focus on methods that generate fast renderings, with at least 15 frames per second to preserve short range motion ([Georgeson and Harris 1990]) necessary to elicit recovery of Structure from Motion ([Dick et al. 1991]). As the underlying algorithms are very costly, requiring intensive per-pixel computations, two approaches can be considered. At first, the development of programmable graphic hardwares (generalized shaders) opens new prospects on the speed of computations. Several works have already been performed in this direction (e.g., [Roettger et al. 2003]). On the other hand, it is possible to reduce the amount of data displayed per image, considering that our attention has limited capacity. For instance, psychological experiments have shown that we are unable to track more than four objects at once, due to the limitation of our attentional system ([Sears and Pylyshyn 2000]). The definition of objects in a volumetric data field can be quite difficult, and it should also not reduce to classical isosurface computations. New methods have to be found to facilitate the analysis of space filling data, and this will be all the more crucial as scientific visualization will face larger and larger amounts of data, due to reduced computational costs: perceptually enhanced visualizations will become one of the major challenges of tomorrow's engineering systems.

The results described in the present paper are tuned to a specific task, the judgment of relative depths of meaningless objects displayed statically or during a 3D motion. Using motion might not always be suitable in the practice of engineers, when static views are likely to facilitate the recognition of specific objects or substructures in the data. The exaggerated perspective we tested in experiment 3 introduces important distortions in shape and size, and might be disturbing when comparing phenomena scattered within the volume. Forthcoming perceptual studies might explore more practical aspects related to volume rendering, such as the accurateness of perception of solid objects embedded in a transparently rendered context.

Future works will include further analysis of our perception of depth in transparent media. In particular, it would be interesting to understand more thoroughly the bias toward seeing large objects in front of smaller ones that was observed in experiment 1. Also, we will clarify the results of experiment 2, and analyze the reasons of the reversal or attenuation of depth perception for dynamic displays with alpha-linear TF. Finally, it is also worth mentioning the development of easier-to-use stereoscopic displays; further experiments exploring the power of stereoscopy in DVR have to be carried out.

Acknowledgments

This work was funded by EDF and a CIFRE grant from Association Nationale de la Recherche Technique. The authors thank the persons who kindly gave time to participate in the experiments.

REFERENCES

Anderson, B. L. 1997. A theory of illusory lightness and transparency in monocular and binocular images: the role of contour junctions. *Perception 26,* 4, 419–453.

Bair, A. and House, D. 2007. Grid with a view: Optimal texturing for perception of layered surface shape. *IEEE Transactions on Visualization and Computer Graphics 13,* 6, 1656–1663.

Bruckner, S. and Gröller, E. 2007. Enhancing depth-perception with flexible volumetric halos. *IEEE Transactions on Visualization and Computer Graphics 13,* 6, 1344–1351.

Dick, M., Ullman, S., and Sagi, D. 1991. Short- and long-range processes in structure-from-motion. *Vision Res 31,* 11, 2025–2028.

Eagle, R. A. and Hogervorst, M. A. 1999. The role of perspective information in the recovery of 3d structure-from-motion. *Vision Res 39,* 9 (May), 1713–1722.

Ebert, D. and Rheingans, P. 2000. Volume illustration: Non-photorealistic rendering of volume models. In *Proceedings Visualization 2000*, T. Ertl, B. Hamann, and A. Varshney, Eds. IEEE Computer Society Technical Committee on Computer Graphics, 195–202.

Engel, K., Kraus, M., and Ertl, T. 2001. High-quality pre-integrated volume rendering using hardware-accelerated pixel shading. In *HWWS '01: Proceedings of the ACM SIGGRAPH/EUROGRAPHICS workshop on Graphics hardware*. ACM Press, New York, NY, USA, 9–16.

Fulvio, J. M., Singh, M., and Maloney, L. T. 2006. Combining achromatic and chromatic cues to transparency. *J Vis 6*, 760–776.

Georgeson, M. A. and Harris, M. G. 1990. The temporal range of motion sensing and motion perception. *Vision Res 30,* 4, 615–619.

Gerbino, W., Stultiens, C. I., Troost, J. M., and de Weert, C. M. 1990. Transparent layer constancy. *J Exp Psychol Hum Percept Perform 16,* 1 (Feb), 3–20.

Giesen, J., Mueller, K., Schuberth, E., Wang, L., and Zolliker, P. 2007. Conjoint analysis to measure the perceived quality in volume rendering. *IEEE Transactions on Visualization and Computer Graphics 13,* 6, 1664–1671.

Green, B. F. 1961. Figure coherence in the kinetic depth effect. *J Exp Psychol 62*, 272–282.

Hibbard, B. 2000. Confessions of a visualization skeptic. *Computer Graphics 34,* 3 (Aug.), 11–13.

Interrante, V., Fuchs, H., and Pizer, S. M. 1997. Conveying the 3D shape of smoothly curving transparent surfaces via texture. *IEEE Trans. Vis. Comput. Graph 3,* 2, 98–117.

Kajiya, J. T. and Herzen, B. P. V. 1984. Ray tracing volume densities. In *SIGGRAPH '84: Proceedings of the 11th annual conference on Computer graphics and interactive techniques*. ACM, New York, NY, USA, 165–174.

Kasrai, R. and Kingdom, F. A. 2001. Precision, accuracy, and range of perceived achromatic transparency. *J Opt Soc Am A Opt Image Sci Vis 18,* 1 (Jan), 1–11.

Kaufman, A. and Mueller, K. 2004. *The Visualization Handbook*. Academic Press, Chapter 7, 127–174.

Kersten, D., Bülthoff, H. H., Schwartz, B. L., and Kurtz, K. J. 1992. Interaction between transparency and structure from motion. *Neural Comput. 4,* 4, 573–589.

Kersten, M., Stewart, J., Troje, N. F., and Ellis, R. E. 2006. Enhancing depth perception in translucent volumes. *IEEE Trans. Vis. Comput. Graph 12,* 5, 1117–1124.

Lacroute, P. and Levoy, M. 1994. Fast volume rendering using a shear-warp factorization of the viewing transformation. In *SIGGRAPH*. ACM, 451–458.

Levoy, M. 1988. Display of surfaces from volume data. *IEEE Computer Graphics and Applications 8,* 3, 29–37.

Masin, S. C. 2006. Test of models of achromatic transparency. *Perception 35,* 12, 1611–1624.

Max, N. 1995. Optical models for direct volume rendering. *IEEE Transactions on Visualization and Computer Graphics 1,* 2, 99–108.

Metelli, F. 1974. The perception of transparency. *Sci Am 230,* 4 (Apr), 90–98.

Mora, B. and Ebert, D. S. 2004. Instant volumetric understanding with order-independent volume rendering. *Comput. Graph. Forum 23,* 3, 489–498.

Nawrot, M. and Blake, R. 1989. Neural integration of information specifying structure from stereopsis and motion. *Science 244,* 4905 (May), 716–718.

Perlin, K. 1985. An image synthesizer. *Computer Graphics 19,* 3 (July), 287–296.

Petersik, J. T. and Dannemiller, J. L. 2004. Factors influencing the ability to detect motion reversals in rotation simulations. *Spat Vis 17,* 3, 201–234.

Pfister, H., Lorensen, B., Schroeder, W., Bajaj, C., and Kindlmann, G. 2000. The transfer function bake-off (panel session). In *VIS '00: Proceedings of the conference on Visualization '00*. IEEE Computer Society Press, Los Alamitos, CA, USA, 523–526.

Roettger, S., Guthe, S., Weiskopf, D., Ertl, T., and Strasser, W. 2003. Smart hardware-accelerated volume rendering.

Rogers, S. and Rogers, B. J. 1992. Visual and nonvisual information disambiguate surfaces specified by motion parallax. *Percept Psychophys 52,* 4 (Oct), 446–452.

Ropinski, T., Steinicke, F., and Hinrichs, K. H. 2006. Visually supporting depth perception in angiography imaging. In *Proceedings of the 6th International Symposium on Smart Graphics (SG06)*. Springer, Vancouver, 93–104.

Sabella, P. 1988. A rendering algorithm for visualizing 3d scalar fields. In *SIGGRAPH '88: Proceedings of the 15th annual conference on Computer graphics and interactive techniques*. ACM Press, New York, NY, USA, 51–58.

Sears, C. R. and Pylyshyn, Z. W. 2000. Multiple object tracking and attentional processing. *Can J Exp Psychol 54,* 1 (Mar), 1–14.

Sereno, M. E. and Sereno, M. I. 1999. 2-d center-surround effects on 3-d structure-from-motion. *J Exp Psychol Hum Percept Perform 25,* 6 (Dec), 1834–1854.

Singh, M. 2004. Lightness constancy through transparency: internal consistency in layered surface representations. *Vision Res 44,* 15, 1827–1842.

Singh, M. and Anderson, B. L. 2002. Toward a perceptual theory of transparency. *Psychol Rev 109,* 3 (Jul), 492–519.

Sperling, G. and Landy, M. S. 1989. Kinetic depth effect and identification of shape. *J Exp Psychol Hum Percept Perform 15,* 4 (Nov), 826–840.

Todd, J. T. 1985. Perception of structure from motion: is projective correspondence of moving elements a necessary condition? *J Exp Psychol Hum Percept Perform 11,* 6 (Dec), 689–710.

Ullman, S. 1979. The interpretation of visual motion. Ph.D. thesis, Mass. Inst. of Technol., Dept. of Elect. Eng. Comput. Sci.

Wallach, H. and O'Connell, D. N. 1953. The kinetic depth effect. *J Exp Psychol 45,* 4 (Apr), 205–217.

A. COMPUTING THE COMPENSATING TRANSLATION IN EXPERIMENT 3

In experiment 3, points in the foreground appear to move faster than those in the background due to perspective foreshortening. Thus, the average projected horizontal speed of the stimulus is biased toward the correct rotation direction, and subjects' decisions might simply reflect this 2D signal, not a true 3D perception. Note however that this effect is weakened by the clipping mask that preserves more points at the background than at the foreground.

To assess this, we implement test trials for the volumetric point cloud in P2 perspective condition. These include an additional horizontal translation of the cylinder opposite to the aforementioned bias. Two speeds of translation are defined: T1 nulls the average projected speed of the point cloud, while T2 equalizes the maximal speed at the foreground and background of the volume. This appendix explicits the formula used to compute the values of T1 and T2.

A point $M(x, y, z)$ (in cylindrical coordinates: $M(\rho cos(\theta), y, \rho sin(\theta))$ within the cylinder is projected on the plane orthogonal to the viewing direction and passing through the center of the cylinder on $Mp(X, Y, 0)$. The center of projection C is

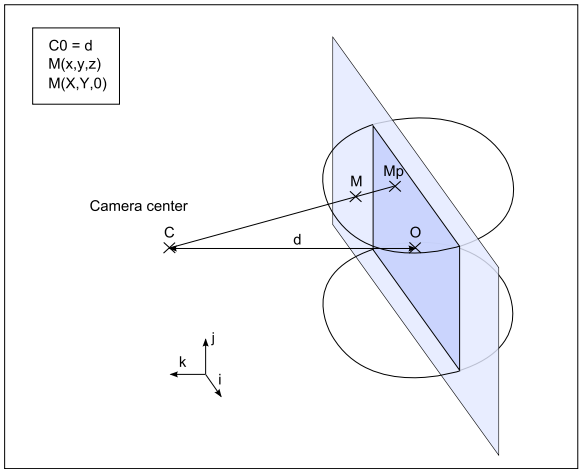

Fig. 11. Notations and reference frame used to compute the amount of translation necessary to null 2D average speed of the stimulus in experiment 3.

positioned at distance d from the center O of the cylinder (radius R), where the reference frame is placed. These notations are depicted in Figure 11.

With $\dot{y} = 0$ for both rotation and translation, Mp position and speed are defined by:

$$Mp \begin{cases} X = x\frac{d}{d-z} \\ Y = y\frac{d}{d-z} \\ Z = 0 \end{cases} \text{ and } \dot{Mp} \begin{cases} \dot{X} = \dot{x}\frac{d}{d-z} + x\dot{z}\frac{d}{(d-z)^2} \\ \dot{Y} = x\dot{z}\frac{d}{(d-z)^2} \\ \dot{Z} = 0 \end{cases} \tag{7}$$

The average motion over the point cloud is the weigthed sum of the unitary mean rotation ($\overline{\dot{X}_R}$) and unitary mean translation ($\overline{\dot{X}_T}$) over the volume:

$$\overline{\dot{X}} = \omega\, \overline{\dot{X}_R} \quad + \quad \delta\, \overline{\dot{X}_T} \tag{8}$$

with:

$$\overline{\dot{X}_R} = \int_{y=-H/2}^{H/2}\int_{\theta=0}^{2\pi}\int_{\rho=0}^{R} -\rho\dot{\theta}\sin(\theta)\frac{d}{d-\rho\sin(\theta)} + \rho^2\dot{\theta}\cos(\theta)^2\frac{d}{(d-\rho\sin(\theta))^2}\,\mathrm{d}\rho\,\mathrm{d}\theta\,\mathrm{d}y \tag{9}$$

$$\overline{\dot{X}_T} = \int_{y=-H/2}^{H/2}\int_{\theta=0}^{2\pi}\int_{\rho=0}^{R} \dot{x}\frac{d}{d-\rho\sin(\theta)}\,\mathrm{d}\rho\,\mathrm{d}\theta\,\mathrm{d}y \tag{10}$$

As these equations are not integrable, and since we must restrict our computations to the points that belong to the visible part of the cylinder (clipped by the four planes defined by the mask, see Figure 8(a)), we relied on a Monte Carlo simulation (10 millions points) to compute the values of ω and δ.